

MILITARY TECHNICAL COLLEGE
CAIRO - EGYPT7th INTERNATIONAL CONF. ON
AEROSPACE SCIENCES &
AVIATION TECHNOLOGY

FINITE DIFFERENCE SOLUTION OF LAMINAR SEPARATED FLOW AROUND A BACK STEP

OSAMA KAMAL*

HAMED ABDALLA**

A. M. SARHAN***

ABSTRACT

In the present work, the computational analysis of laminar, incompressible separated flow over a backstep is introduced by solving the incompressible Navier-Stokes equations. The technique of vorticity transport equation and Poisson equation are used to calculate the velocity through the domain, then the Poisson equation for pressure is used to get the value of the pressure all over the domain. Obtained data are graphically presented. Smoke wind tunnel is used to trace the flow streak lines around a finite length flat plate with backstep. Qualitative comparison between calculated and experimentally obtained traces showed good agreement.

KEY WORDS

Computational Fluid Dynamic \ Finite Difference \ Flow separation \ Wake.

1 INTRODUCTION

Flow separation over and behind a finite body has always been an important problem for the flying bodies. This separation creates a wake zone of high vorticity and negative pressure. Consequently, it causes drag. Even for streamlined surfaces (wings) flow separation occurs at high angles of attack. This reduces the lift and increases the drag of these aerodynamic surfaces. In the early forties Schlichting [1], could analytically investigate the wake problem. Later on, Nayfeh [2], and Dyke [3] separately established the fundamentals of the perturbation technique which could render better solution of the wake problem. In the last three decades, due to the rapid progress of the computing machines, increased attention has been paid to the numerical solutions of the flow separation, [4-10].

For some viscous flow problems, as in the present case of study (wake flow); the solution of the complete set of Navier-Stokes equations becomes necessary. Unfortunately, these equations are very complex and require a substantial amount of computer time in order to obtain an accurate solution. However, if the flow is incompressible, the equations can be considerably simplified. Consequently, the required computer time is decreased. The unsteady, incompressible N.S. equations are a mixed set of elliptic-parabolic equations. In order to explain the time step limitation, all the explicit methods solving the compressible N.S. equations are limited to a time step; Anderson, D.A., [11]; which is less than that given by the Courant, Friedrichs and Lewy (CFL) condition. As a result, an infinitely large amount of

* M.Sc., Department of Rockets, MTC, CAIRO, EGYPT.

** Assoc.Prof., Chairman of the Department of Rockets, MTC, CAIRO, EGYPT.

*** Assoc.Prof., Department of Rockets, MTC, CAIRO, EGYPT.

computer time would be required to compute a truly incompressible flow in this manner. On the other hand, implicit methods permit larger Δt , but the maximum value; as stated by Anderson, D.A., [11]; is normally about 5:10 times that given by CFL otherwise truncation errors become unacceptable.

2 THEORETICAL ANALYSIS

2.1 Primitive Equations

The incompressible Navier-Stokes equations for a constant property flow without body forces nor external heat addition are given in the vector form as:

Continuity $\nabla \cdot \mathbf{V} = 0$

Momentum $\rho \frac{D\bar{\mathbf{V}}}{Dt} = -\nabla p + \mu \nabla^2 \mathbf{V}$

Energy $\rho c_v \frac{DT}{Dt} = K \nabla^2 T + \Phi$

Where \mathbf{V} , Φ , K , T , μ , ρ , and c_v are the velocity vector, dissipation function, coefficient of thermal conductivity, temperature, dynamic viscosity, fluid density and specific heat at constant volume, respectively.

These equations are a mixed set of elliptic-parabolic equations which contain the unknowns (\mathbf{V} , p , T). Since the temperature appears only in the energy equation, therefore it can be uncoupled from the continuity and momentum equations. Moreover, in the present case of study, the temperature changes are unimportant, consequently, the energy equation will not be solved at all. The 2-D incompressible Navier-Stokes equations using the **primitive-variable form**, are:

Continuity $\frac{\partial \bar{u}}{\partial x} + \frac{\partial \bar{v}}{\partial y} = 0$ (1)

X Momentum $\frac{\partial \bar{u}}{\partial t} + \bar{u} \frac{\partial \bar{u}}{\partial x} + \bar{v} \frac{\partial \bar{u}}{\partial y} = \frac{-1}{\rho} \frac{\partial \bar{p}}{\partial x} + \nu \left(\frac{\partial^2 \bar{u}}{\partial x^2} + \frac{\partial^2 \bar{u}}{\partial y^2} \right)$ (2)

Y Momentum $\frac{\partial \bar{v}}{\partial t} + \bar{u} \frac{\partial \bar{v}}{\partial x} + \bar{v} \frac{\partial \bar{v}}{\partial y} = \frac{-1}{\rho} \frac{\partial \bar{p}}{\partial y} + \nu \left(\frac{\partial^2 \bar{v}}{\partial x^2} + \frac{\partial^2 \bar{v}}{\partial y^2} \right)$ (3)

Where, the overbars represent the dimensional quantities of the velocity components in x and y directions, respectively.

2.2 Stream Function and Vorticity Transport Equations

In the present work, the Vorticity-Stream function approach have been utilized by replacing the primitive variables with stream function ψ and the vorticity ξ , where the stream function ψ is defined as:

$$\bar{u} = \frac{\partial \bar{\psi}}{\partial y} \quad \text{and} \quad \bar{v} = - \frac{\partial \bar{\psi}}{\partial x} \quad (4)$$

while, for 2-D flow, the vorticity is expressed as

$$\bar{\xi} = \frac{\partial \bar{v}}{\partial x} - \frac{\partial \bar{u}}{\partial y} \quad (5)$$

The pressure is eliminated from Eq.2 and Eq.3 then, one can obtain the **vorticity transport equation** expressed in the conservative form as

$$\frac{\partial \bar{\zeta}}{\partial t} = -\bar{v} \cdot (\bar{v}\bar{\zeta}) + \bar{v}\bar{\nabla}^2 \bar{\zeta} = - \left(\frac{\partial(\bar{u}\bar{\zeta})}{\partial \bar{x}} + \frac{\partial(\bar{v}\bar{\zeta})}{\partial \bar{y}} \right) + \bar{v} \left(\frac{\partial^2 \bar{\zeta}}{\partial \bar{x}^2} + \frac{\partial^2 \bar{\zeta}}{\partial \bar{y}^2} \right) \quad (6)$$

The vorticity transport Eq.6 is a parabolic equation. It consists of the unsteady term $\partial \bar{\zeta} / \partial t$, the advective terms $\partial(\bar{u}\bar{\zeta}) / \partial \bar{x} + \partial(\bar{v}\bar{\zeta}) / \partial \bar{y}$, and the viscous diffusion term $\bar{v} \left(\partial^2 \bar{\zeta} / \partial \bar{x}^2 + \partial^2 \bar{\zeta} / \partial \bar{y}^2 \right)$.

Eq.5 is recasted as an elliptic *Poisson equation*

$$\nabla^2 \bar{\psi} = -\bar{\zeta} \quad (7)$$

2.3 Normalized System

The normalized system used, is based on the advective time scale \bar{L} / \bar{u}_∞ , where \bar{L} and \bar{u}_∞ are the characteristic length (boundary layer thickness) and the free stream velocity respectively. The dimensionless parameters are defined as:

$$\begin{aligned} u &\equiv \bar{u} / \bar{u}_\infty, \quad v \equiv \bar{v} / \bar{u}_\infty, \quad x \equiv \bar{x} / \bar{L}, \quad y \equiv \bar{y} / \bar{L}, \\ \zeta &\equiv \bar{\zeta} / (\bar{u}_\infty / \bar{L}), \quad t \equiv \bar{t} / (\bar{L} / \bar{u}_\infty), \quad p \equiv \bar{p} / \rho \bar{u}_\infty^2 \end{aligned} \quad (8)$$

Hence, the *Vorticity Transport* equation and the *Poisson equation* take the following dimensionless form:

$$\frac{\partial \zeta}{\partial t} = -\nabla \cdot (v \cdot \zeta) + \frac{1}{Re} \nabla^2 \zeta \quad (9)$$

$$\nabla^2 \psi = -\zeta \quad (10)$$

where, Re, is the Reynolds number, $Re \equiv \bar{u}_\infty \bar{L} / \nu$

Thus, for any well posed boundary condition, the flow is described by a single dimensionless parameter which is the Reynolds number.

2.4 Solution of The Vorticity-Stream Function

Since the case of study is a 2-D flow problems, the vorticity-stream function approach will be used because it is easy to solve two equations rather than three equations. Also, it is possible to separate the mixed elliptic-parabolic 2-D, incompressible Navier-Stokes equations into one parabolic equation (Vorticity Transport equation), and one elliptic equation (Poisson equation).

In the present case of study, the time-dependent behavior is not required, but only the steady state solution, which being obtained from the time dependent equations as the asymptotic time limit of the unsteady equations.

The steps of solution are described as:

- 1- Discretize the partial differential equations into difference equations.
- 2- Pose the boundary conditions.
- 3- Specify initial conditions and initial guessed values for ζ and ψ at time $t = 0$.
- 4- Calculate new time $t = t + \Delta t$.
- 5- Find new ζ by solving the vorticity transport equation for ζ at each interior grid point at time $t + \Delta t$.
- 6- Iterate for new ψ values at all points by solving the Poisson equation using the calculated new ζ at interior points.
- 7- Find the velocity components from Eq. 4
- 8- Determine values of ζ on the boundaries using new ψ and ζ values at interior points.

9- If the solution is not converged to a steady state solution; Return to step 4, until convergence occurs.

During solution the velocity components are determined at each grid point. By the end of these steps, the values of u , v , ψ , and ζ are completely determined all over the domain. To determine the pressure at each grid point, it is necessary to solve an additional equation which is referred to as the *Poisson equation for pressure*, Roache,[12]

$$\nabla^2 p = 2\rho \left(\frac{\partial u}{\partial x} \frac{\partial v}{\partial y} - \frac{\partial v}{\partial x} \frac{\partial u}{\partial y} \right) \quad (11)$$

In terms of the stream function this equation can be expressed as

$$\nabla^2 p = S = 2\rho \left\{ \left(\frac{\partial^2 \psi}{\partial x^2} \right) \left(\frac{\partial^2 \psi}{\partial y^2} \right) - \left(\frac{\partial^2 \psi}{\partial x \partial y} \right)^2 \right\} \quad (12)$$

3.0 NUMERICAL ANALYSIS

The finite difference technique is adapted to solve for the flow parameters behind a backstep of finite length.

3.1 Finite Difference Scheme

The domain is discretized into mesh points; Fig.1. The backstep corner has a position of I_C and J_C in the x and y directions, respectively. The velocity components are obtained from the stream function values by centered differencing of Eq.4. While the vorticity equation will be discretized as:

$$\zeta_{i,j}^{k+1} = \zeta_{i,j}^k + \Delta t \left\{ -\frac{\partial(u\zeta)^k}{\partial x_{i,j}} - \frac{\partial(v\zeta)^k}{\partial y_{i,j}} + \frac{1}{\text{Re}} \left(\frac{\partial^2 \zeta^k}{\partial x_{i,j}^2} + \frac{\partial^2 \zeta^k}{\partial y_{i,j}^2} \right) \right\} \quad (13)$$

The diffusion terms are represented by the usual centered difference form. The advection terms are represented by using the suggested scheme by Wirz, [13]

$$\frac{\partial(u\zeta)^k}{\partial x_{i,j}} = \frac{u_R \zeta_R - u_L \zeta_L}{\Delta x} \quad (14)$$

where the subscript R and L stands for right to and left from the mesh point of interest, respectively, such that

$$u_R = 0.5(u_{i+1,j} + u_{i,j}) \quad \text{and} \quad u_L = 0.5(u_{i,j} + u_{i-1,j}) \quad (15)$$

$$\zeta_R = \begin{cases} \zeta_{i,j} & \text{for } u_R > 0 \\ \zeta_{i+1,j} & \text{for } u_R < 0 \end{cases} \quad \& \quad \zeta_L = \begin{cases} \zeta_{i-1,j} & \text{for } u_L > 0 \\ \zeta_{i,j} & \text{for } u_L < 0 \end{cases} \quad (16)$$

and the same for $\partial(v\zeta)^k / \partial y_{i,j}$. In this differencing method, information is advected into any cell from those cells that are upwind of it.

The linear stability analysis suggests a critical time step above which dynamic instability will be anticipated, Roache, [1976].

$$\Delta t_{\text{crit}} \leq \left(\left(\frac{2}{\text{Re}} \right) \left(\frac{1}{\Delta x^2} + \frac{1}{\Delta y^2} \right) + \frac{|u_{i,j}|_{\text{max}}}{\Delta x} + \frac{|v_{i,j}|_{\text{max}}}{\Delta y} \right)^{-1} \quad (17)$$

To insure stability, only a fraction of this critical time step is used, usually 85:95% of the critical time step $\Delta t_{\text{critical}}$, Roache, [12], and Wirz, [13]. In the present work, a value 95% is used.

The Poisson equation is discretized, using the Successive Over Relaxation, SOR, method, Roache and Muller, [4], as follows:

$$\psi_{i,j}^{k+1} = \psi_{i,j}^k + \frac{\omega}{2(1+\beta^2)} \left\{ \psi_{i+1,j}^k + \psi_{i-1,j}^{k+1} - 2(1+\beta^2)\psi_{i,j}^k + \zeta_{i,j} \Delta x^2 + \beta^2 (\psi_{i,j-1}^{k+1} + \psi_{i,j+1}^k) \right\} \quad (18)$$

Where, ω is the relaxation factor. For convergence, it is required that $1 \leq \omega \leq 2$. The optimum value ω_o , depends on the mesh size, the shape of the domain and the type of the boundary conditions, Roache [12].

$$\omega_o = 2 \left(\frac{1 - \sqrt{1-f}}{f} \right) \quad (19)$$

$$f = \left[\left(\cos \left(\frac{\pi}{I_{\max} - 1} \right) + \beta^2 \cos \left(\frac{\pi}{J_{\max} - 1} \right) \right) / (1 + \beta^2) \right]^2 \quad (20)$$

where β , I_{\max} & J_{\max} are the grid ratio ($\Delta x/\Delta y$), number of the grid point in x and y direction, respectively.

3.2 Numerical Boundary Conditions for Vorticity-Stream Function

The present case of study is a boundary value problem. Therefore, it is important to specify the boundary conditions, giving a special care to the corner (point of singularity).

The computational domain has six boundaries; Fig.2; B_1 , B_2 , B_3 , B_4 , B_5 and B_6 are the upstream boundary, horizontal surface, vertical backstep surface, center line of the backstep, far down stream (outlet) boundary and the far free stream boundary.

3.2.1 The upstream boundary B_1

The velocity profile, $u(y)$, used at inflow boundary is the Pohlhausen fourth order polynomial profile results from the integral solution of the boundary-layer equations, Roache and Mueller, [4]

$$u(B_1) = (2\eta - 2\eta^3 + \eta^4) + \frac{\Lambda}{6} (\eta - 3\eta^2 + 3\eta^3 - \eta^4) \quad (21)$$

where

η , Ratio of the height of the point of interest to the boundary layer thickness, $\eta = y/\delta$.

Λ , Pohlhausen parameter, $\Lambda \equiv \frac{-dp}{dx} \frac{\delta^2}{\mu u}$. In the absence of pressure gradient, $\Lambda = 0$.

To obtain the stream function ψ at the inlet, in a compatible manner with the velocity differencing as in $u_{0,j} = 0.5 (\psi_{0,j+1} - \psi_{0,j-1})/\Delta y$, this gives

$$\psi_{0,jc} = 0, \quad \psi_{0,jc+1} = 0.5 u_{0,jc+1} \Delta y \quad \& \quad \psi_{0,j} = 2 \Delta y u_{0,j-1} + \psi_{0,j-2} \quad (22)$$

The subscript c stands for the corner, and 0 stands for the first mesh point, at $x=0$.

The velocity v at inlet is calculated from the continuity equation

$$v_{0,j} = v_{0,j-1} + \frac{u_{0,j} - u_{1,j}}{\beta} \quad (23)$$

Since in the present work, the viscous effect is important at the input and it is desirable to fix $u_{0,j}$ and to let $v_{0,j}$ develop freely. Thus, the upstream inflow boundary is partly determined by specifying a boundary layer inflow, and partly develops as a part of the solutions.

3.2.2 The wall boundaries, B₂ and B₃

Since the line B₂-B₃ represents a stream line, so any constant value of the stream function might be used. The conventional choice is $\psi = 0$. The vorticity is obtained from the no slip condition, using the boundary B₂ as an example, $\psi_{i,jc+1}$ is expanded; by a Taylor series; out from the wall values $\psi_{i,jc}$ as:

$$\psi_{i,jc+1} = \psi_{i,jc} + \left. \frac{\partial \psi}{\partial y} \right|_{i,jc} \Delta y + \left. \frac{\partial^2 \psi}{\partial y^2} \right|_{i,jc} \frac{\Delta y^2}{2} + \dots \quad (24)$$

From the no-slip condition, $u = v = 0$, consequently, $u_{i,jc} = \partial \psi / \partial y|_{i,jc} = 0$

Hence,
$$\left. \frac{\partial^2 \psi}{\partial y^2} \right|_{i,jc} = \frac{2(\psi_{i,jc+1} - \psi_{i,jc})}{\Delta y^2} \quad (25)$$

Since, $v=0$ along the horizontal wall, consequently, $\partial v / \partial x|_{i,jc} = 0$. By substituting in Eq.5, the vorticity will be

$$\zeta = -\frac{\partial u}{\partial y} = -\frac{\partial}{\partial y} \left(\frac{\partial \psi}{\partial y} \right) = -\frac{\partial^2 \psi}{\partial y^2} \quad (26)$$

By substituting in Eq.25, the value of the vorticity is obtained at the wall as:

$$\zeta = -2(\psi_{i,jc+1} - \psi_{i,jc}) / \Delta y^2 \quad (27)$$

Hence, regardless of the wall orientation or the value of ψ at the wall, the vorticity at the wall will be

$$\zeta_{\text{wall}} = -2(\psi_{\text{wall}+1} - \psi_{\text{wall}}) / \Delta n^2 \quad (28)$$

where, Δn is the distance normal to the wall from the (wall) to (wall+1).

3.2.3 The center line boundary B₄

Since the backstep geometry presents the symmetrical half of the base flow problem, then, $\psi = 0$. So, the velocity u is determined by extrapolation from interior point

$$u_{i,0} = 2u_{i,1} - u_{i,2} \quad (29)$$

Since, u is symmetric about the center line; $\partial u / \partial y = 0$; thus from Eq.5,

$$\zeta_{\text{c.L.}} = 0. \quad (30)$$

3.2.4 The far down stream boundary B₅

Assuming that $\partial \zeta / \partial x = 0$, and $\partial v / \partial x = 0$ at the far outlet, and since $v = -\partial \psi / \partial x$, this second condition implies that $\partial^2 \psi / \partial x^2 = 0$ which was approximated by linear extrapolation out to $i = I_{\text{max}}$. For constant Δx this gives

$$\zeta_{I \text{ max}} = 2 \zeta_{I \text{ max}-1} - \zeta_{I \text{ max}-2}, \quad \psi_{I \text{ max}} = 2 \psi_{I \text{ max}-1} - \psi_{I \text{ max}-2}$$

$$u_{I \text{ max},j} = (\psi_{I \text{ max},j+1} - \psi_{I \text{ max},j-1}) / 2 \Delta y \quad \text{and} \quad v_{I \text{ max},j} = (\psi_{I \text{ max}-1,j} - \psi_{I \text{ max},j}) / \Delta x \quad (31)$$

where, I_{max} is the farthest grid point in the x direction.

3.2.5 The far free stream boundary B₆

The most nearly free stream condition found is to use an *impermeable* slip wall at the lid. The value of ψ is set from the inflow boundary conditions as:

$$\psi_{\text{lid}} = \psi_{0,J \text{ max}} \quad \text{and} \quad \zeta_{i,J \text{ max}} = \zeta_{i,J \text{ max}-1} \quad (32)$$

$$v_{i,J \text{ max}} = 0 \quad \text{and} \quad u_{i,J \text{ max}} = 2 u_{i,J \text{ max}-1} - u_{i,J \text{ max}-2} \quad (33)$$

i.e., u is found by a linear extrapolation from interior point out to the lid.

3.2.6 The sharp corner

Since the corner is a point of singularity, therefore it requires especial careful treatment. The stream function ψ at the sharp corner like the rest of the wall, which means that $\psi_c=0$. The vorticity at the corner is evaluated by using a discontinuous value for ζ_c . Applying the wall Eq.28 to the horizontal wall, a value of $\zeta_c=\zeta_a$ is obtained and by doing this to the downstream wall (vertical wall) a value of $\zeta_c=\zeta_b$ is obtained. So, when ζ_c is used in the difference equations at node (I_c, J_c+1) , just above the corner, then $\zeta_c = \zeta_a$ is used. While when using ζ_c in the difference equations at node (I_c+1, J_c) , then $\zeta_c = \zeta_b$ is used.

3.3 Pressure Solution

Solving the Vorticity-Stream function equations, the values of u , v , ψ , and ζ all over the domain is specified. So it is required to extract the pressure solution from the numerical solution. The pressure equation to be used is the Poisson equation of pressure, identical to the equation for stream function, but a major difficulty arises in the use of the SOR iteration method because of the boundary conditions are of different types. To obtain the pressure values, we start at an arbitrary point with an arbitrary pressure level; constant of integration; and numerically integrate the discretized momentum equations for $\partial p/\partial x$ and $\partial p/\partial y$.

Poisson Equation of Pressure

The Poisson equation of pressure, Anderson, D. A., [11], and Roache, [12] is

$$\frac{\partial^2 p}{\partial x^2} + \frac{\partial^2 p}{\partial y^2} = S = 2 \left\{ \left(\frac{\partial^2 \psi}{\partial x^2} \right) \left(\frac{\partial^2 \psi}{\partial y^2} \right) - \left(\frac{\partial^2 \psi}{\partial x \partial y} \right)^2 \right\} \quad (34)$$

Its finite difference form is

$$p_{i,j}^{k+1} = \frac{1}{2(1+\beta^2)} \left\{ p_{i+1,j}^k + p_{i-1,j}^{k+1} + \beta^2 (p_{i,j-1}^{k+1} + p_{i,j+1}^k) - S_{i,j} \Delta z^2 \right\} \quad (35)$$

where

$$S_{i,j} = 2 \left(\left(\frac{\psi_{i+1,j} + \psi_{i-1,j} - 2\psi_{i,j}}{\Delta x^2} \right) \left(\frac{\psi_{i,j+1} + \psi_{i,j-1} - 2\psi_{i,j}}{\Delta y^2} \right) - \left(\frac{\psi_{i,j+1} - \psi_{i,j-1} - \psi_{i-1,j+1} + \psi_{i-1,j-1}}{2\Delta x \Delta y} \right) \right) \quad (36)$$

Eq.34 is analogous to the stream function equation; Eq.12; with the source term S analogous to ζ .

According to Anderson, D.A., [11], there are two methods for the solution. The first is the *Pressure surface solution*, which produces the pressure values at the solid surfaces only. The second is the *Pressure domain solution* (iterative solution method), which produces the values of the pressure at the whole investigated domain

Roache, [12], mentioned that the first method gives different answers when different paths are used. This method is susceptible to errors especially in problems like that of the present case of study when the path of integration is close to a sharp convex corner. So, in the present work, the second method is used.

3.3.2 Pressure domain solution method (Iterative Solution Method)

To get the values of the pressure, the surrounding domain is divided into two portions, Figure 2, each of them is treated with its own equations. The first portion is the mesh points

which are located on the boundaries. While the second portion contains all the interior points which are located at more than one node from the boundaries.

At the first portion, the boundaries, the normal derivative for pressure is calculated and then incorporated directly into the SOR difference scheme. For the horizontal wall, as for example

$$p_{i,jc}^{k+1} = p_{i,jc+1}^{k+1} - \Delta y \frac{\partial p}{\partial y} \quad (37)$$

$$p_{i,jc}^{k+1} = p_{i,jc}^k + \frac{\omega}{2 + \beta^2} \left\{ p_{i+1,jc}^k + p_{i-1,jc}^{k+1} - (2 + \beta^2) p_{i,jc}^k - \beta^2 \left(p_{i,jc+1}^k - \Delta y \frac{\partial p}{\partial y} \right) - S_{i,jc} \Delta x^2 \right\} \quad (38)$$

While at the second portion, the interior points, the values of the pressure are calculated from the SOR method directly.

$$p_{i,j}^{k+1} = p_{i,j}^k + \frac{\omega}{2(1 + \beta^2)} \left\{ p_{i+1,j}^k + p_{i-1,j}^{k+1} - 2(1 + \beta^2) p_{i,j}^k + \beta^2 (p_{i,j+1}^k + p_{i,j-1}^{k+1}) - S_{i,j} \Delta x^2 \right\} \quad (39)$$

So the steps of solution for pressure is as follows

- 1- Calculate $\partial p / \partial n$ at all boundaries, then compute the values of the pressure p on the boundaries as a function of $\partial p / \partial n$ and the interior points.
- 2- Solve the Poisson's equation, Eq.35; for the pressure at the interior points.
- 3- There is a fixed point in the domain, reference point, having a constant value for pressure $p=1.0$. Its location is one node down from the upper boundary and one node after the inlet, $i=1$; Fig. 2; then calculate $\Delta p = p_{ref,calculated} - p_{reference}$.
- 4- The value of the pressure at each grid point is calculated from $p_{i,j} = p_{i,j} - \Delta p$
- 5- The error in pressure is calculated, $\epsilon_p = |p_{i,j}^{k+1} - p_{i,j}^k|$ at each point in the domain.
- 6- Store the maximum value for ϵ_p
- 7- Compare the calculated error; ϵ_p ; with the required degree of accuracy. If not achieved, return to step 1. In the present work, the value needed for convergence was, $\epsilon_p = 5 \times 10^{-5}$.

3.3.3 boundary conditions

In the solution of the vorticity equation $\nabla^2 \psi = -\zeta$, at least some of the boundary conditions were of the first kind, Dirichlet boundary condition, where $\psi(x,y)$ was specified along the boundaries. Meanwhile, in the solution of the Poisson equation of the pressure, the boundary conditions are of the second kind, Neumann boundary conditions, specifying $\partial p / \partial n(x,y)$, where n is a direction normal to the boundary of interest. The values of the pressure gradients are found from the momentum equation.

The upstream boundary B₁

Using the x momentum equation, noting that for a steady state, $\partial / \partial t = 0$, hence

$$\frac{\partial p}{\partial x} = \frac{1}{\text{Re}} \left(\frac{\partial^2 u}{\partial x^2} + \frac{\partial^2 v}{\partial y^2} \right) - u \frac{\partial u}{\partial x} - v \frac{\partial u}{\partial y} \quad (40)$$

By assuming that the second derivative of the velocity u does not vary over the first two levels of the grid points; $\partial^2 u / \partial x^2 \Big|_{i=0} = \partial^2 u / \partial x^2 \Big|_{i=1}$; then the x momentum equation will take the finite difference form as:

$$\left. \frac{\partial p}{\partial x} \right|_{i=0,j} = -u_{0,j} \frac{u_{1,j} - u_{0,j}}{\Delta x} - v_{0,j} \left(\frac{u_{0,j+1} - u_{0,j-1}}{2\Delta y} \right) + \frac{1}{\text{Re}} \left(\frac{u_{0,j+1} + u_{0,j-1} - 2u_{0,j}}{\Delta y^2} + \frac{u_{2,j} + u_{0,j} - 2u_{1,j}}{\Delta x^2} \right) \quad (41)$$

So, the pressure at the boundary B₁ will be $\frac{\partial p}{\partial x} = \frac{p_{1,j} - p_{0,j}}{\Delta x}$

hence, $p_{i-1,j} = p_{i,j} - \Delta x \frac{\partial p}{\partial x}$ (42)

i.e. $p_{0,j} = p_{1,j} - \Delta x \frac{\partial p}{\partial x}$ (43)

Using Gauss Sidle method; Eq.35 and Eq.36 gives

$$p_{i,j}^{k+1} = \frac{1}{1 + 2\beta^2} \left\{ p_{i+1,j}^k - \Delta x \left. \frac{\partial p}{\partial x} \right|_{i,j} + \beta^2 (p_{i,j-1}^{k+1} + p_{i,j+1}^k) - S_{i,j} \Delta x^2 \right\} \quad (44)$$

$$S_{i,j} = 2 \left(\left(\frac{\psi_{2,j} + \psi_{0,j} - 2\psi_{1,j}}{\Delta x^2} \right) \left(\frac{\psi_{0,j+1} + \psi_{0,j-1} - 2\psi_{0,j}}{\Delta y^2} \right) - \left(\frac{\psi_{1,j+1} - \psi_{1,j-1} - \psi_{0,j+1} + \psi_{0,j-1}}{2\Delta x \Delta y} \right) \right) \quad (45)$$

Then the SOR method is used to get the value of the pressure

$$p_{i,j}^{k+1'} = p_{i,j}^k + \omega (p_{i,j}^{k+1} - p_{i,j}^k) \quad (46)$$

where

p^k The value from the previous iteration as adjusted by previous application of this formula.

p^{k+1} The most recent value of, p, calculated from the Gauss-sidle.

$p^{k+1'}$ The newly adjusted or "better guessed value", for p at k+1 iteration level.

The horizontal wall B₂

Using the y momentum equation; the pressure gradient will be:

$$\left. \frac{\partial p}{\partial y} \right|_{\text{Horizontal wall}} = \frac{1}{\text{Re}} \frac{\partial \zeta}{\partial x} = \frac{1}{\text{Re}} \frac{\zeta_{i+1,j} - \zeta_{i-1,j}}{2\Delta x} \quad (47)$$

By substituting in the Poisson equation of pressure; Eq.35 reduces to

$$p_{i,j}^{k+1} = \frac{1}{2 + \beta^2} \left\{ p_{i+1,j}^k + p_{i-1,j}^{k+1} + \beta^2 \left(p_{i,j+1}^k - \Delta y \left. \frac{\partial p}{\partial y} \right|_{i,j} \right) - S_{i,j} \Delta x^2 \right\} \quad (48)$$

The SOR method; Eq.46; is used to get the values of the pressure at horizontal surface

The vertical wall B₃

Since at the vertical wall $\partial u / \partial y = 0$, then by using the x momentum equation, the axial pressure gradient will be

$$\left. \frac{\partial p}{\partial x} \right|_{\text{vertical wall}} = \frac{-1}{\text{Re}} \left(\frac{\partial \zeta}{\partial y} \right) \quad (49)$$

by substituting in the Poisson equation of the pressure

$$p_{i,j}^{k+1} = \frac{1}{1+2\beta^2} \left\{ p_{i+1,j}^k - \Delta x \frac{\partial p}{\partial x} + \beta^2 (p_{i-1,j}^{k+1} + p_{i,j+1}^k) - S_{i,j} \Delta x^2 \right\} \quad (50)$$

The SOR method, Eq.46, is used to get the pressure values at the vertical surface

The Center Line B₄

Since, the center line is a line of symmetry, then $\partial p / \partial y = 0$, and since $\partial^2 \psi / \partial x^2 = 0$
 $S = -2(\partial^2 \psi / \partial x \partial y)^2$, which takes the following finite difference form

$$S_{i,0} = -2 \left(\frac{\psi_{i+1,1} - \psi_{i-1,1} - \psi_{i+1,0} + \psi_{i-1,0}}{2\Delta x \Delta y} \right)^2 \quad (51)$$

since, $\partial p / \partial y = 0$, then $p_{i,j-1}^{k+1} = p_{i,j}^{k+1}$ (52)

Therefore, the Poisson equation for the pressure will be

$$p_{i,j}^{k+1} = \frac{1}{1+2\beta^2} \left\{ p_{i+1,j}^k + p_{i-1,j}^{k+1} + \beta^2 p_{i,j+1}^k - S_{i,j} \Delta x^2 \right\} \quad (53)$$

For the SOR method; Eq.46; is used to get the pressure values at the center line.

The Far Downstream Boundary (outlet) B₅

Using the X momentum equation, and by assuming that the second derivative does not vary over the last two grids in x direction, i.e. $\partial^2 u / \partial x^2 \Big|_{i=I \max} = \partial^2 u / \partial x^2 \Big|_{i=I \max-1}$, Then the finite difference equation will be

$$\frac{\partial p}{\partial x} \Big|_{i=I,j} = -u_{I,j} \frac{3u_{I,j} - 4u_{I-1,j} + u_{I-2,j}}{2\Delta x} - v_{I,j} \left(\frac{u_{I,j+1} - u_{I,j-1}}{2\Delta y} \right) + \frac{1}{\text{Re}} \left(\frac{u_{I,j+1} + u_{I,j-1} - 2u_{I,j}}{\Delta y^2} + \frac{u_{I-2,j} + u_{I,j} - 2u_{I-1,j}}{\Delta x^2} \right) \quad (54)$$

where, I is the maximum value for i, (at the last mesh point).

hence, $p_{i+1,j} = p_{i,j} + \Delta x \frac{\partial p}{\partial x}$. Using Gauss Sidle method, then

$$p_{i,j}^{k+1} = \frac{1}{1+2\beta^2} \left\{ p_{i-1,j}^{k+1} + \Delta x \frac{\partial p}{\partial x} + \beta^2 (p_{i,j-1}^{k+1} + p_{i,j+1}^k) - S_{i,j} \Delta x^2 \right\} \quad (55)$$

The central difference form will be used to introduce the finite difference form for S. Where $\partial^2 \psi / \partial x^2$ is applied at $I=I \max-1$, while $\partial^2 \psi / \partial y^2$ and $\partial^2 \psi / \partial x \partial y$ are applied at $I=I \max$. Then the SOR method, Eq.46, is used to get the values of the pressure.

The far free stream boundary (the lid) B₆

Using the y momentum equation while $\partial^2 v / \partial x^2$, $\partial v / \partial y$ and $\partial v / \partial x$ are applied at $j=J \max$ while $\partial^2 v / \partial y^2$ is applied at $j=J \max-1$

since $\frac{\partial p}{\partial y} = \frac{p_{i,J \max} - p_{i,J \max-1}}{\Delta y}$ then, $p_{i,j+1} = p_{i,j} + \Delta y \frac{\partial p}{\partial y}$

By substituting in the Poisson equation of the Pressure, Eq.39, to get the values of the pressure

$$p_{i,j}^{k+1} = \frac{1}{2+\beta^2} \left\{ p_{i+1,j}^k + p_{i-1,j}^{k+1} + \beta^2 \left(p_{i,j-1}^k + \Delta y \frac{\partial p}{\partial y} \right) - S_{i,j} \Delta x^2 \right\} \quad (56)$$

Since ψ is constant through the lid, this implies that $\partial^2\psi/\partial x^2=0$, then, $S = -2(\partial^2\psi/\partial x\partial y)^2$. So, the finite difference form will be the same as Eq.51, but with $j = J_{\max}$, then the SOR method is used to get the values of the pressure.

The Sharp Corner

Since the corner is a point of singularity, it will be treated as if it was two separate points with an infinitesimal distance separating them, the same treatment as in the $\psi-\zeta$ solution, P_a belongs to the horizontal surface, while the other point P_b belongs to the vertical one. So, there will be two values of pressure at the corner, Roache, [12]

Calculation of P_a

Using the x momentum equation just at the corner and at the point just leading to it

$$\frac{\partial p}{\partial x} = - \frac{1}{Re} \frac{\partial \zeta}{\partial y}$$

$$\left. \frac{\partial p}{\partial x} \right|_{ic} = \frac{-1}{Re} \left(\frac{-3\zeta_{ic,j} + 4\zeta_{ic,j+1} - \zeta_{ic,j+2}}{2\Delta y} \right)$$

$$\left. \frac{\partial p}{\partial x} \right|_{ic-1} = \frac{-1}{Re} \left(\frac{-3\zeta_{ic-1,j} + 4\zeta_{ic-1,j+1} - \zeta_{ic-1,j+2}}{2\Delta y} \right)$$

then $\left. \frac{\partial p}{\partial x} \right|_a = 0.5 \left(\left. \frac{\partial p}{\partial x} \right|_{ic} + \left. \frac{\partial p}{\partial x} \right|_{ic-1} \right)$ (57)

so, $P_a = P_{ic-1,j} + \Delta x \left. \frac{dp}{dx} \right|_a$ (58)

Calculation of P_b

Using the y momentum equation, at the corner and at the point just below it using the same procedure as in the case of P_a .

3.4 Error Calculation And Convergence Criteria

At every grid point, the error is calculated as $\epsilon_x = |X_{i,j}^{k+1} - X_{i,j}^k|$ where X stands for ψ , ζ , and p, then taking the maximum value across the whole domain, this value must not exceed a certain value which is the solution degree of accuracy wanted. If this value is not achieved then another iteration takes place until the required value is achieved. ψ is permitted to use only a finite number of iterations; 5 iterations; not to reach a certain error. It gives very good accuracy and a limited total iteration numbers. At the end, the solution satisfies the error for both ψ and ζ .

In the present work the value of the error for Stream Function ψ , is 10^{-8} , Vorticity ζ is 10^{-7} , while for Pressure p is 5×10^{-5}

4 RESULTS

In the present case of study, the presented results are obtained for the following parameters: flow over back step with sharp corner, no axial pressure gradient, computational field with rectangular shape of 60 grid height and 150 grid in the longitudinal direction. 20 x 20 cell corner, grid ratio $\beta=2.0$, where $\Delta x=0.1$ and $\Delta y=0.05$, $\Delta t_{crit}=0.95\Delta t$, $Re=100$. The inflow boundary layer thickness $\delta/h=1$, where h is the backstep height. The inflow condition was

located at two base heights upstream of the corner and the free stream was at two base heights above the corner.

Obtained data are graphically presented as follows:

Fig. 3, represents the error course for the stream function ψ , the vorticity ζ and the sum of stream function. The error is strongly converging without any oscillation which is the advantage of the ψ - ζ approach. The sum of the stream function all over the domain behaves as a constant value near convergence. The behavior of the two methods ensure convergence of the solution

Fig. 4, represents the error course of the Poisson equation of pressure. Convergence occurs faster than ψ - ζ solution.

Fig. 5, represents the contour plots for ψ , ζ , c_p and the stagnation pressure at Reynolds number = 100.

Fig. 5-a, is a contour plot of the stream function. The increased spacing between the streamlines at constant $\Delta\psi$ indicates lower volumetric flux in the lower portions of the boundary layer, consequently lower velocity. The extrapolated separation point occurs less than one cell below the sharp corner, and reattachment occurs at mesh point number 124 in the x direction, i.e., at 10.4 base height downstream of the corner.

Fig. 5-b, is a contour plot of the vorticity. The heavy concentration of contour lines near the sharp corner indicates high vorticity gradient in this region. Within the upstream boundary layer, the constant vorticity lines generally follow the streamline shapes. Outside the boundary layer, no vorticity contour lines appear, indicating a region of nearly zero vorticity.

Fig. 5-c, is a contour plot of the pressure coefficient, where $c_p \equiv (p-p_\infty)/q_0$ and $q_0 = 0.5(u^2+v^2)_{\text{ref}}$ is a dimensionless dynamic pressure at the reference position. The plot shows that c_p is equal to zero at the beginning of the horizontal surface, then, it decreases and has a negative values. When approaching the corner and in the base region, where the lowest value of c_p is located, positive pressure drag of the backstep due to the viscous pumping effect is indicated. As advancing far from the backstep the value of c_p increases, until at $i=110$, i.e. at 11 base height, the value of c_p reaches zero again, then it continue increasing to reach a positive value. The pressure in the downstream region is nearly one-dimensional, as indicated by the nearly vertical contour lines. This implies that $\partial p/\partial y \approx 0$. Also at the inflow, the departure from the boundary-layer assumption $\partial p/\partial y = 0$ is small, and appears to be due to the upstream influence of the corner. In the corner and base region, the pressure field is strongly two-dimensional. The calculated average base pressure coefficient over the vertical surface is equal to -0.077

Fig. 5-d, is a contour plot of the stagnation pressure, $P_T = P + 0.5(u^2 + v^2)$. The gradient regions of P_T are seen to be confined with the viscous regions, with very little variation of P_T above the boundary layer and the free shear layer. In the boundary layer P_T generally follows the streamlines.

The obtained data showed good agreement when compared to that obtained by Roache, [4].

5 EXPERIMENTAL VERIFICATION

A short model with a length of 12.2 cm, width of 2.3 cm, and thickness of 2.6 cm is manufactured. The leading edge of the model is rounded to avoid flow separation. The width of the model is obligatory small to fit the test section. The test model is qualitatively tested in a smoke wind tunnel. The photo of the test model, presented in Fig.(6), show the phenomenon of the flow separation at the trailing edge of the model. The smoke trace (streak line) is similar to the steady state stream function, obtained by numerical calculation, presented in Fig.(5-a). When the flow speed increases; consequently the Reynolds number; the flow separation starts earlier and its length is increased, Fig.(7). This confirms the obtained numerical results.

6 CONCLUSIONS

The presented work is a contribution to the numerical analysis of the flow separation. A versatile computer program is coded to solve for the flow field around a finite plate with backstep.

REFERENCES

1. Schlichting, (1979), *Boundary Layer Theory*, McGraw-Hill.
2. Nayfeh, A. H., [1973], *Perturbation Methods*, John Wiley & Sons.
3. Dyke, M. V., [1975], *Perturbation Methods in Fluid Mechanics*, The Parabolic Press.
4. Roache, P. J., and Muller, T. J., March (1970), " *Numerical Solutions of Laminar Separated Flows* ", AIAA Journal, Vol. 8, No. 3.
5. Merz, R. A., Yi, C. H. and Prziembel, C. E. G., October (1985), " *The Subsonic Near-Wake of an Axisymmetric Semielliptical After body* ", AIAA Journal, Vol. 23, No. 10, pp. 1512-1517.
6. Ozlem Ilday, Hary Acar, M. Kubilay Elbay and Veysel Atli, June (1993), " *Wakes of Three Axisymmetric Bodies at Zero Angle of Attack* ", AIAA Journal, Vol. 31, No. 6, pp. 1152-1154.
7. Veysel Atli, June (1989), " *Wakes of Four Complex Bodies of Revolution at Zero Angle of Attack* ", AIAA Journal, Vol. 27, No. 6, pp. 707-711.
8. Hirsch, C., (1990), *Numerical Computation of Internal and External Flows*, Vol. 1 and 2, John Wiley & Sons.
9. Osama Kamal, (1995), " *Computational Technique for Drag Calculation* ", M.Sc. Thesies, MTC.
10. Osama Kamal, Hamed Abdalla, Sarhan, A.M., " *Numerical solution of laminar separated flow over the base of a cylinder* ", 7th applied mechanics and mechanical engineering conference, MTC, Cairo, EGYPT, 1996.
11. Anderson, D. A., Tannhill, J. C., and Pletcher, R. H., (1984), *Computational Fluid Mechanics and Heat Transfer*, McGraw-Hill.
12. Roache, P. J., (1976), *Computational Fluid Dynamics*, Hermosa Publishers.
13. Wirz, H. J. and Smoldern, J. J., (1978), *Numerical Methods in Fluid Dynamics*, McGraw-Hill.

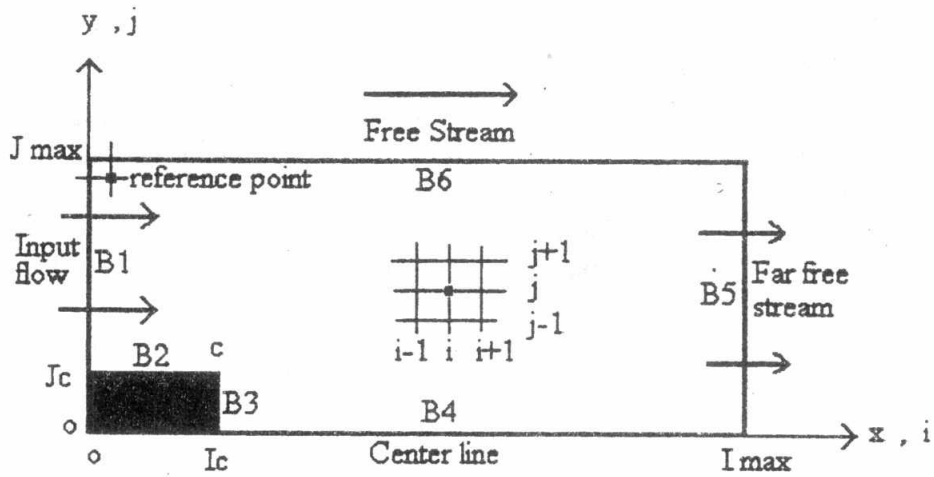


Figure 1 Boundary layer labels used.

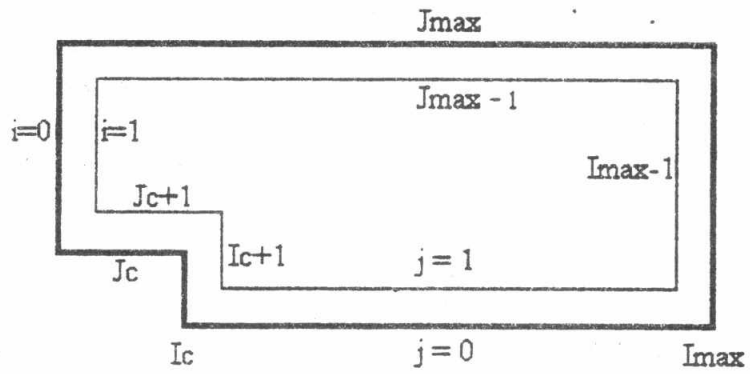


Figure 2 Domain portions for the pressure solution.

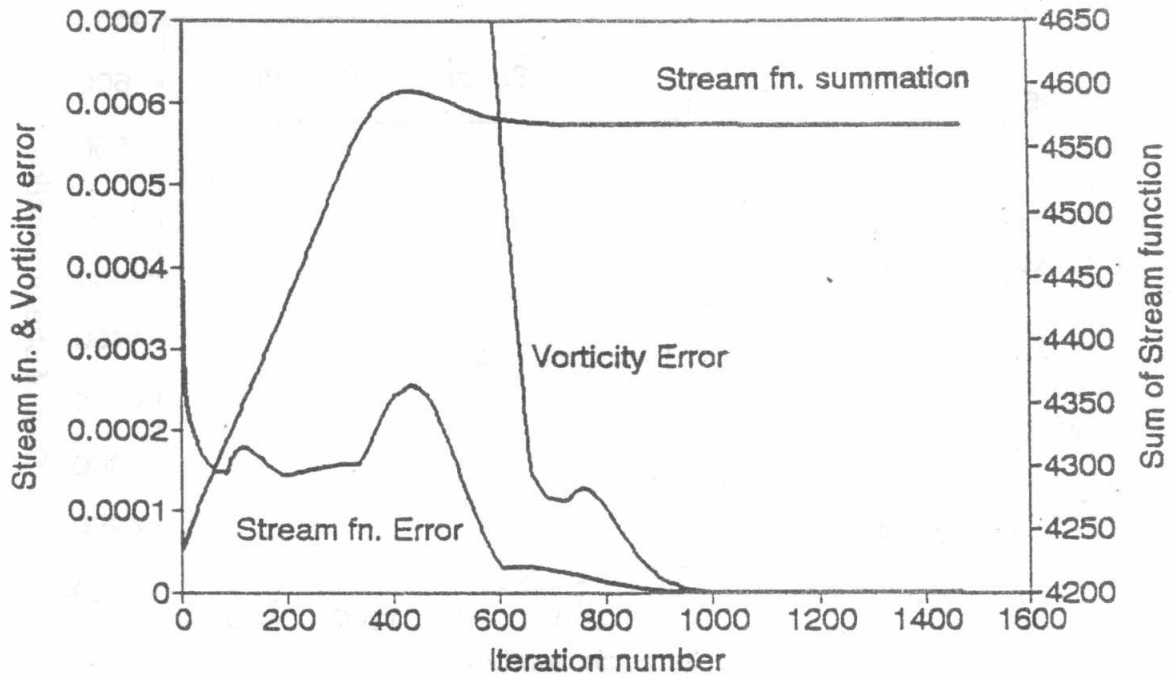


Figure 3, Error course for the stream function and vorticity equation for laminar, incompressible flow over a backstep, $Re = 100$

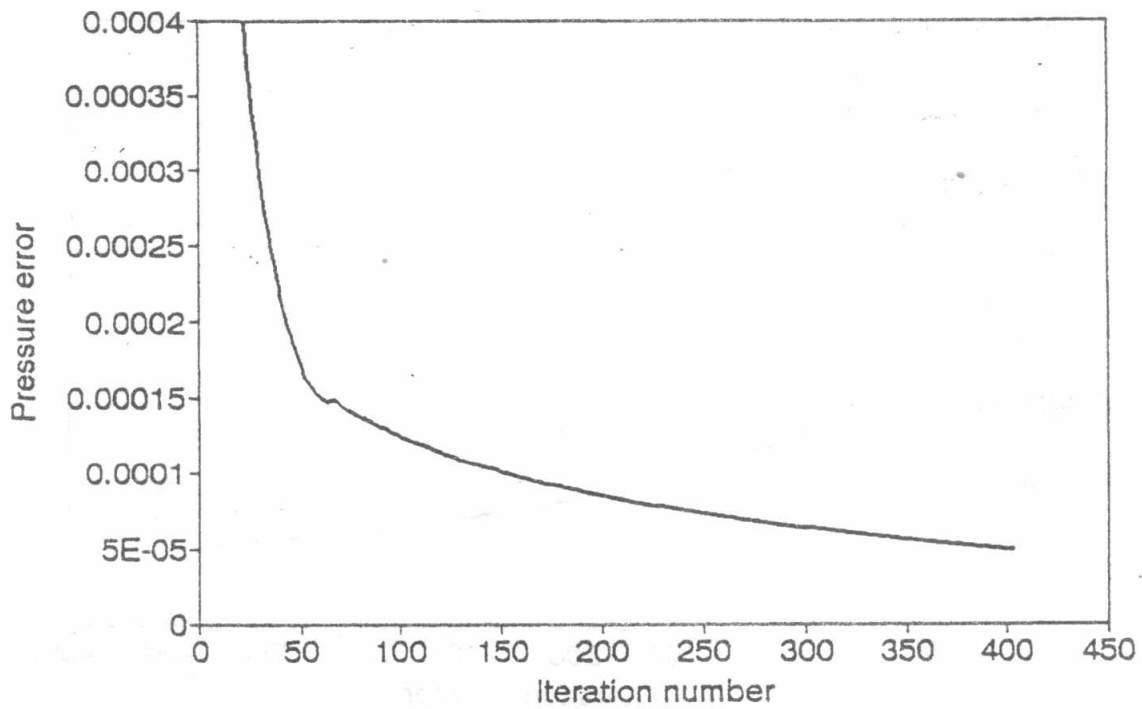


Figure 3, Error course for the Poisson's equation for pressure for laminar, incompressible flow over a backstep, $Re = 100$

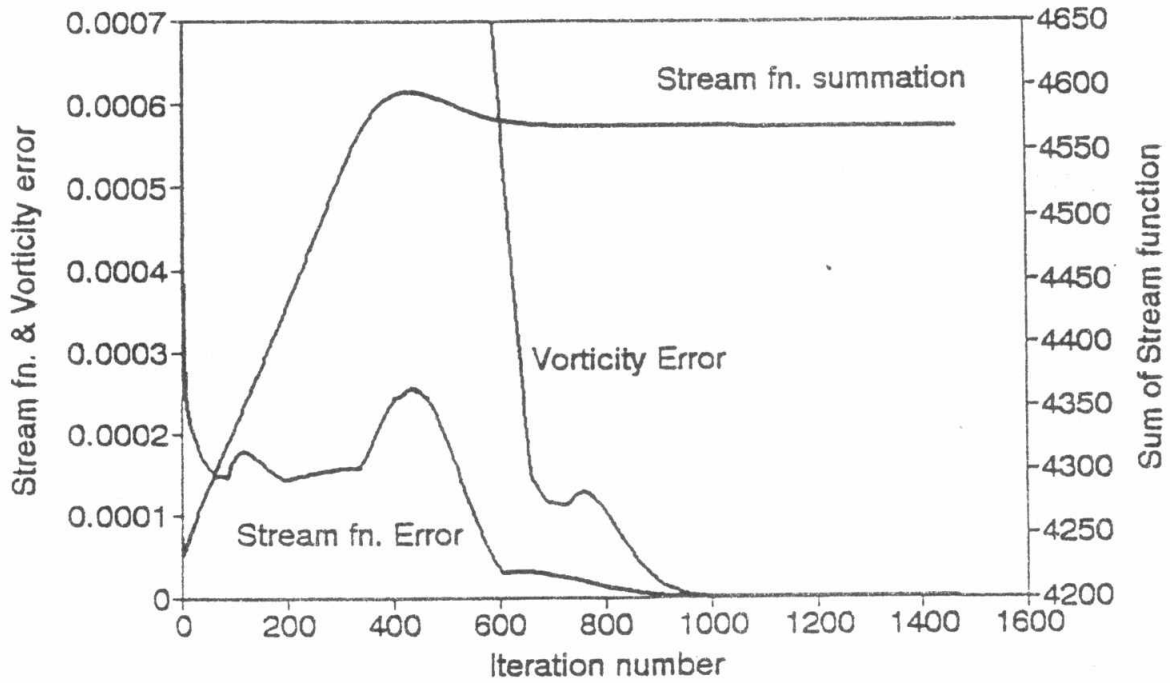


Figure 3, Error course for the stream function and vorticity equation for laminar, incompressible flow over a backstep, $Re = 100$

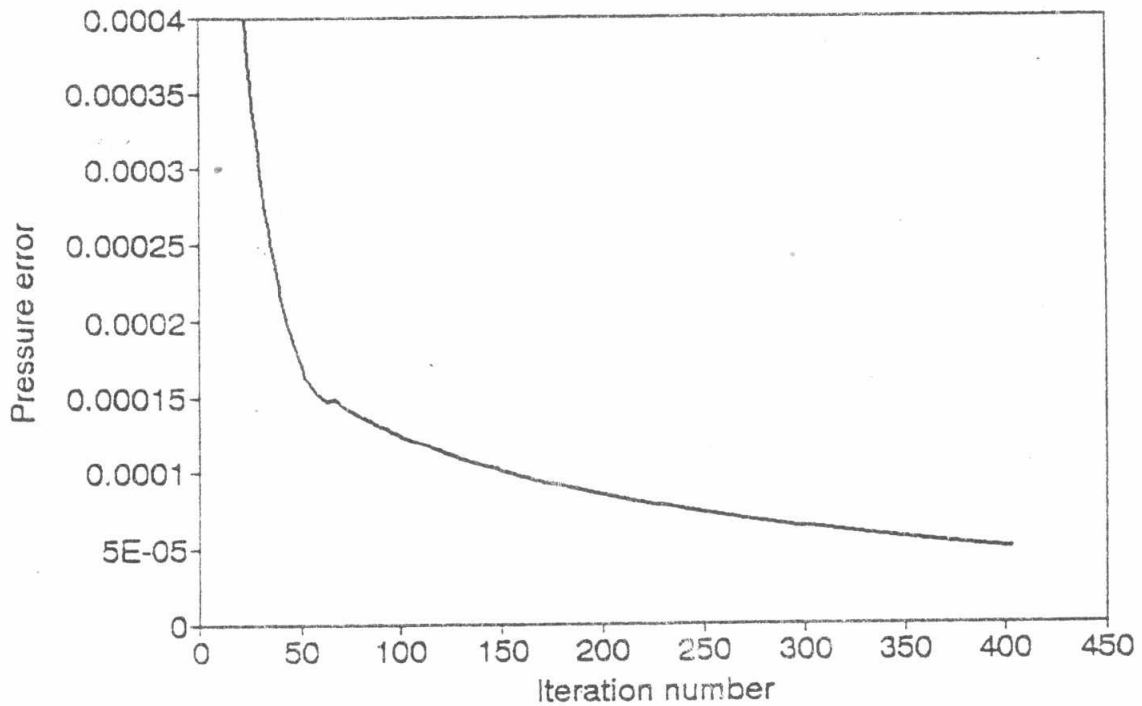


Figure 4, Error course for the Poisson's equation for pressure for laminar, incompressible flow over a backstep, $Re = 100$

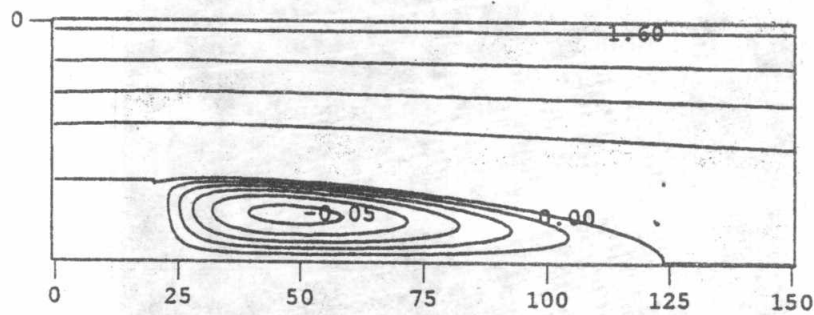


Fig. 5-a Stream Function

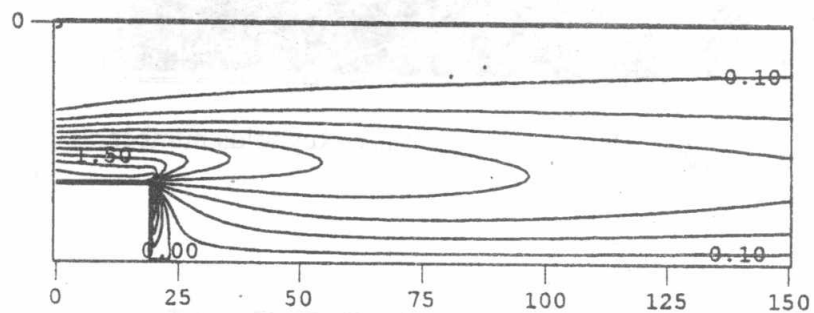


Fig. 5-b Vorticity

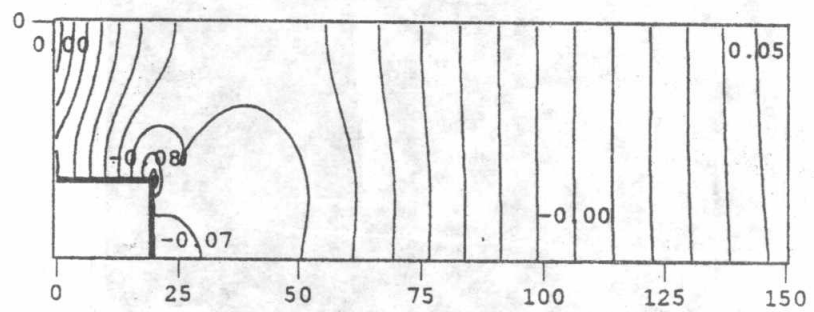


Fig. 5-c Pressure coefficient

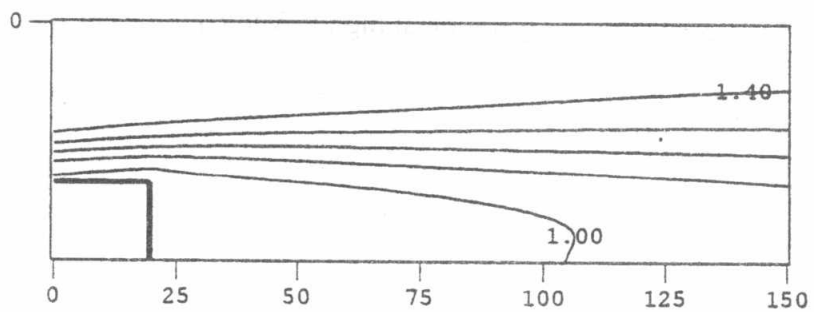


Fig. 5-d Stagnation pressure

Figure 5 Incompressible, laminar flow over a backstep at $Re = 100$,
 $\Delta\psi = 0.4$ above $\psi = 0.0$, $\Delta\psi = 0.01$ below $\psi = 0.0$, $\Delta\zeta = 0.1$ above
 $\zeta = 0.0$, $\Delta\zeta = 0.2$ below $\zeta = 0.0$, $\Delta C_p = 0.01$ above and below
 $C_p = 0.0$, $\Delta P_T = 0.1$

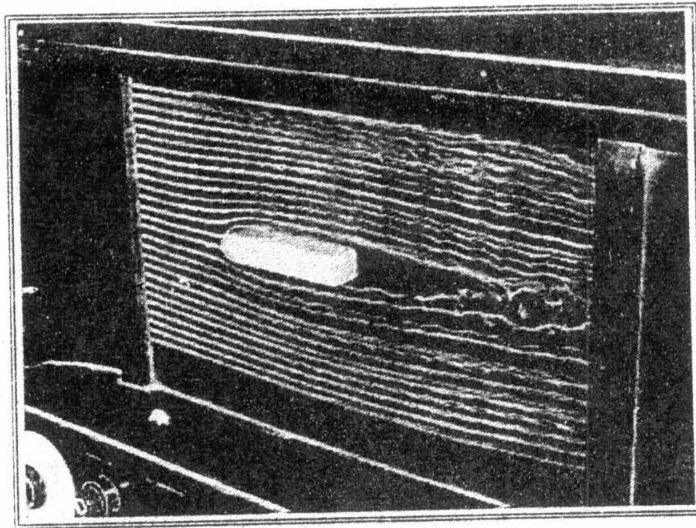


Figure 6 Flow separation at low Reynolds number.

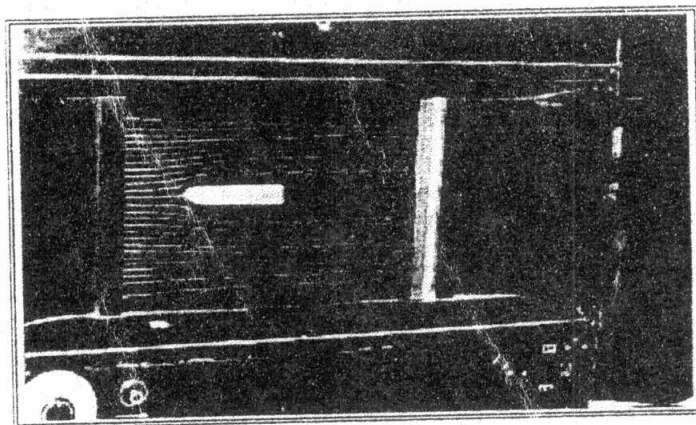


Figure 7 Flow separation at high Reynolds number.